ARTICLE NO. 79-1646R

Alleviation of Vortex-Induced Asymmetric Loads

L.E. Ericsson* and J.P. Reding†
Lockheed Missiles & Space Company, Inc., Sunnyvale, Calif.

The existing experimental data base for vortex-induced asymmetric loads has been reviewed with special emphasis on the asymmetric vortices generated by a slender nose. The results indicate that micro-asymmetrics on a slender nose determine the downstream development of asymmetric vortices. Consequently, the asymmetric vortex shedding can most effectively be changed by devices active at or near apex. The alleviation effect can be accomplished either by delayig all vortex shedding through the use of nose bluntness, or by extending the angle-of-attack range for symmetric vortex shedding utilizing strakes or body trips.

Nomenclature

A	= axial force: coefficient $C_A = A/(\rho_\infty U_\infty^2/2)S$
$C_{m\alpha}$	$= \partial C_m/\partial\alpha$
$C_{n\beta}$	$= \partial C_n/\partial\beta$
c	= reference length ($c=d$)
d	= maximum diameter of body of revolution
l	= body length
M	= Mach number
M_p	= pitching moment: coefficient $C_m = M_p/(\rho_\infty U_\infty^2/2)Sc$
n	= yawing moment: coefficient $C_n = n/(\rho_\infty U_\infty^2/2)Sc$
N	= normal force: coefficient $C_N = N/(\rho_\infty U_\infty^2/2)S$
p	= static pressure: coefficient $C_p = (p-p_\infty)/(\rho_\infty U_\infty^2/2)$
r	= body radius
Re, R_d	= Reynolds number $= U_\infty d/\nu_\infty$
S	= reference area $= \pi d^2/4$
U	= horizontal velocity
x	= axial body-fixed coordinate (distance from apex)
Y	= side force: coefficient $C_Y = Y/(\rho_\infty U_\infty^2/2)S$
α	= angle of attack
β	= sideslip angle
θ_c	= cone half-angle
θ_A	= apex half-angle
ρ	= air density
ϕ	= roll angle
ν	= kinematic viscosity

Subscripts

A	= apex
B	= base
c	= cone
N	= nose
∞	= freestream conditions

Introduction

At high angles of attack the flow separating off the leeside of a slender body rolls up into a pair of symmetric vortices. Above some critical high angle of attack the vortices become asymmetric, generating large side forces that can cause an aircraft to spin or a missile to tumble, if these vortex effects have not been considered in the control design. Although the phenomenon has been known for some time,[1-5] it was of little practical interest until recently when both high-performance aircraft and missiles began operating at these high angles of attack.

That the lateral loads induced by asymmetric vortex shedding at zero sideslip give cause for concern is illustrated by Figs. 1 and 2. The results[6] in Fig. 1 show that at high angles of attack the vortex-induced side force can exceed the normal force on a pointed missile body. The data[7] in Fig. 2 demonstrate that the vortex-induced side loads on an advanced performance aircraft can exceed the available control capability by one order of magnitude. Figure 2 also illustrates that it is difficult to make sure that the experiment reveals what the maximum possible side load can be. For that reason a method has been developed[8,9] which can predict the upper bounds for the vortex-induced side force and associated side moment. These loads may exceed the control capability, or the pitch-yaw-roll coupling provided by the asymmetric vortices[10,11] may be unacceptable. In either case a design fix of some form is needed. The present paper discusses means to eliminate or greatly reduce the asymmetric vortex effects without unduly compromising vehicle stability and performance.

Discussion

Asymmetric vortex shedding has been observed to start on slender, pointed noses when the angle of attack exceeds the total included angle at the apex,[12,13] i.e., when $\alpha \geq 2\theta_A$. For not so slender noses ($\theta_A > 20$ deg) the first asymmetric vortex starts on the cylindrical aft body at station x when $\alpha \approx 4.2\, d/x$ according to Fiechter's results.[5] This is in basic agreement with the findings by Keener et al.[12,14] The dominating influence of the apex illustrated by the results[2,15] in Figs. 3 and 4 has been observed by numerous investigators. All these results indicate rather strongly that minute model asymmetries at the nose control the vortex asymmetry. Lamont and Hunt[16] suspected wind-tunnel turbulence to be an equally likely source. However, when their test was repeated in a low-turbulence (0.01%) tunnel,[17] the results showed that turbulence was not a factor. All available evidence indicated that

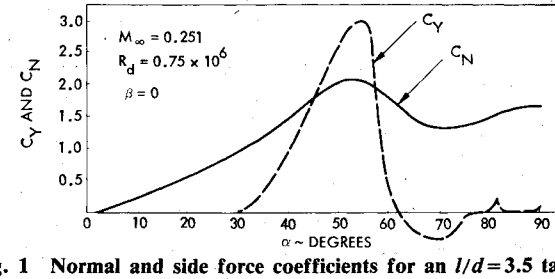

Fig. 1 Normal and side force coefficients for an $l/d = 3.5$ tangent ogive.[6]

Presented as Paper 79-1646 at the AIAA Atmospheric Flight Mechanics Conference, Boulder, Colo., Aug. 6-8, 1979; submitted Oct. 26, 1979; revision received April 1, 1980.

Index categories: LV/M Aerodynamics; Jets, Wakes, and Viscid-Inviscid Flow Interactions; Subsonic Flow.

*Senior Consulting Engineer. Associate Fellow AIAA.
†Staff Engineer. Associate Fellow AIAA.

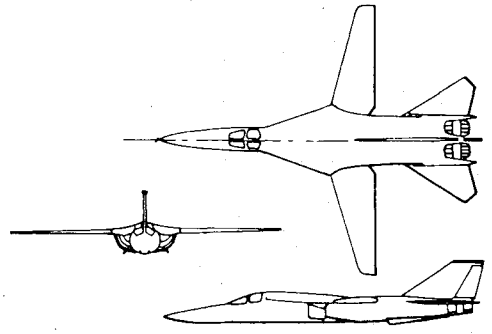

Three-view sketch of configuration with long pointed nose

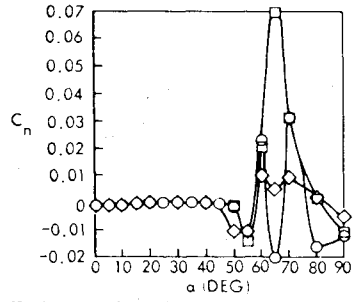

a) Variation of yawing-moment coefficient with angle-of-attack, symbols indicate values obtained in several repeat tests

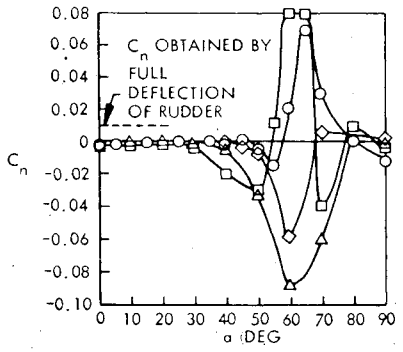

b) Variation of static yawing-moment coefficient with angle-of-attack for several models of the configuration, $\beta = 0$ deg.

Fig. 2 Repeated measurements of vortex-induced yawing moment on an aircraft.[7]

micro-asymmetries at the nose tip controlled the formation of asymmetric vortices.

Gower and Perkins[2] showed that one way to alleviate the formation of asymmetric vortices was to blunt the sharp conic nose tip. Adding a nose boom[12,18] has also been shown to delay the early formation of asymmetric vortices (Fig. 5). The boom generates its own vortex wake that could "bury" the micro-asymmetrics at the apex, thereby delaying the asymmetric vortex formation. If the apex is blunted, the nose boom no longer has any effect on the vortex-induced side loads.[12] Pick found in his investigation[19] that small nose bluntness (<25%) had a dramatically alleviating effect on the side load (Fig. 6). The results obtained by Coe et al.[20] also show this beneficial effect of nose bluntness. The results in Ref. 12 show that the large side force on a pointed ogive can be eliminated almost completely by the use of 4.2, 8.4, or 16.7% hemispherical nose bluntness.

Thus, the most effective means of controlling the body vortices is to interfere with the initial vortex generation at or near the apex. This is also true for delta-wing vortices where apex rounding has been found to delay their formation greatly.[21] Also in regard to the effect of nose bluntness it seems to be the planform of the nose roundness that counts,

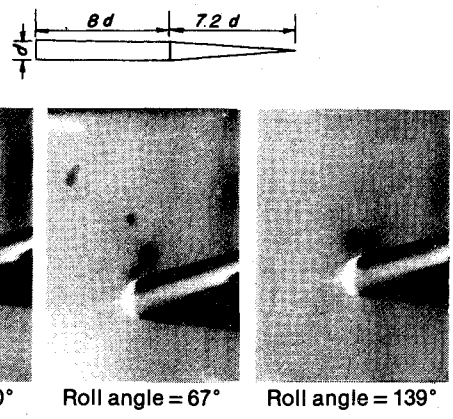

Fig. 3 Effect of tip rotation on asymmetric vortex formation on a cone-cylinder at $l/d = 3.75$.[2]

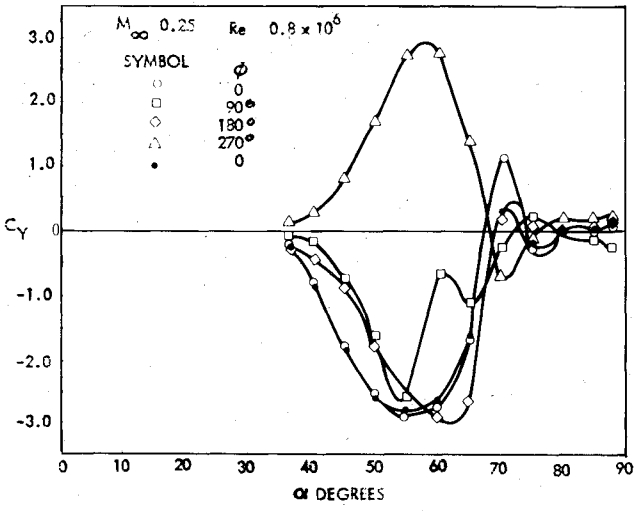

a) Effect of body roll angle

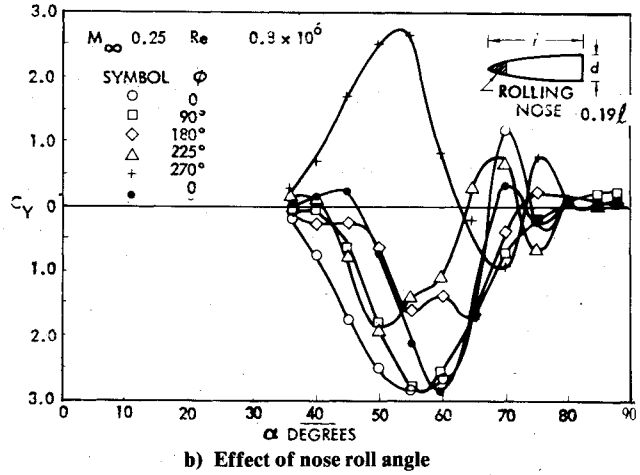

b) Effect of nose roll angle

Fig. 4 Effect of roll angle on vortex-induced side force on an $l/d = 3.5$ tangent ogive.[15]

as is indicated by the results obtained by Titiriga and Skow for the slender nose of an aircraft[22] (Fig. 7). One somewhat surprising trend in Pick's data[19] is that if the nose bluntness is larger than 25% (e.g., 50%) the side force becomes large again (Fig. 6). One wonders naturally why. Our thoughts on the subject are as follows. When the nose is slender ($\theta_A < 20$ deg) the first asymmetric vortex pair is generated on the nose, and sets the pattern for additional vortex generation on the cylindrical aft body, as is indicated by the results by

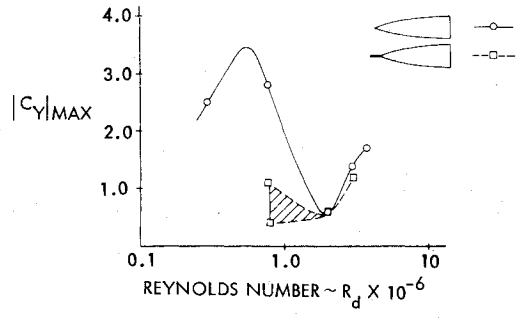

Fig. 5 Effect of nose boom on the side-force of an $l/d = 3.5$ pointed tangent ogive.[12]

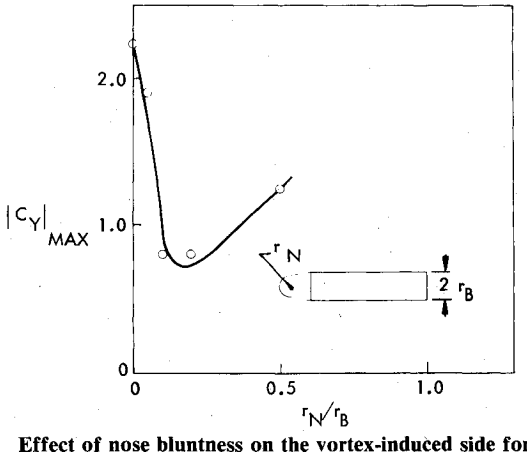

Fig. 6 Effect of nose bluntness on the vortex-induced side force on an ogive-cylinder.[19]

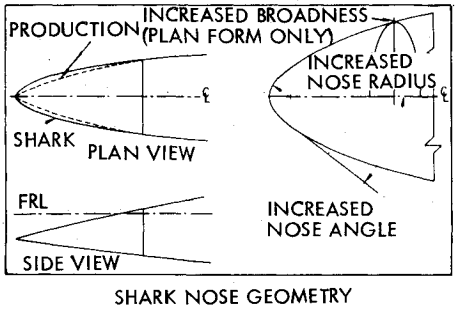

SHARK NOSE GEOMETRY

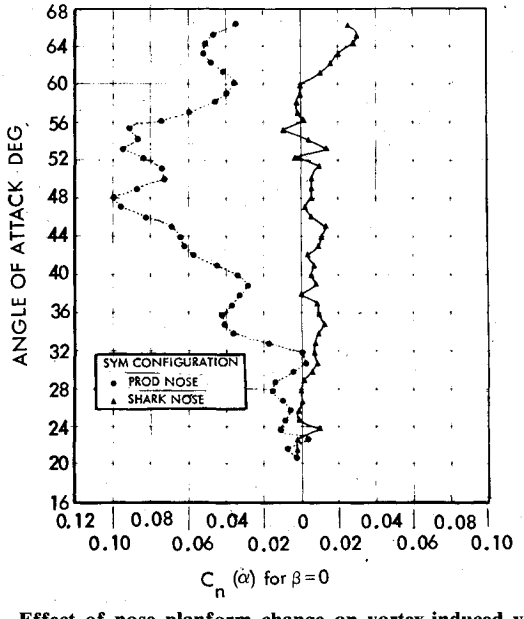

Fig. 7 Effect of nose planform change on vortex-induced yawing moment.[22]

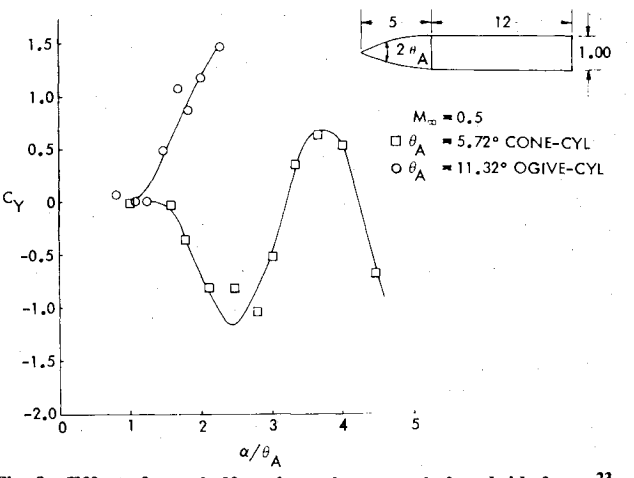

Fig. 8 Effect of apex half-angle on the vortex-induced side force.[23]

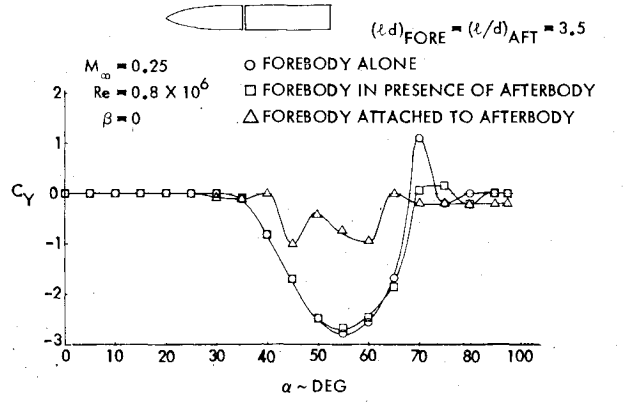

Fig. 9 Effect of cylindrical aft body on the vortex-induced side force of an $l/d = 3.5$ pointed tangent ogive.[12]

Atraghji[23] (Fig. 8) and Keener and Chapman[12] (Fig. 9). Figure 8 shows that it is not the nose slenderness ratio that counts, which is 5 for both the conic and ogival nose, but that it is rather the apex angle. The data in Fig. 9 show the same dominating influence of the asymmetric vortex pattern generated at the apex. Thus, the asymmetric vortices on the aft body, although producing a substantial decrease in the overall net side force, do not influence the vortex-asymmetry on the nose but rather "line up" in the pattern already set by the nose vortices.

This dominance of the nose-generated vortices shows why nose bluntness exerts such an overriding influence over the side force. Small nose bluntness delays the asymmetric vortex formation on the nose thereby decreasing the vortex-induced side force. Eventually, as the nose bluntness is increased, the nose will become too short to support asymmetric vortex formation. Thus, the first asymmetric vortex pair is generated by the cylinder, not by the nose. The existence of a single vortex pair brings back the large side force, e.g., for 50% nose bluntness in Fig. 6.

There is no doubt about the efficiency of small nose bluntness in reducing the maximum vortex-induced side force on an airplane fuselage or a short missile body. However, on very long bodies nose blunting may actually increase $|C_Y|_{max}$. The reason for this is as follows: For a pointed slender nose the asymmetric vortex shedding starts very early. Consequently, at large angles of attack, where the vortex-induced loads maximize, a pointed long body will contain many asymmetric vortex cells. In contrast, a blunter nose can, due to the delay of the start of asymmetric vortices, generate its first asymmetric vortex pair at a much larger angle of attack and hence can have a single vortex pair at a very large

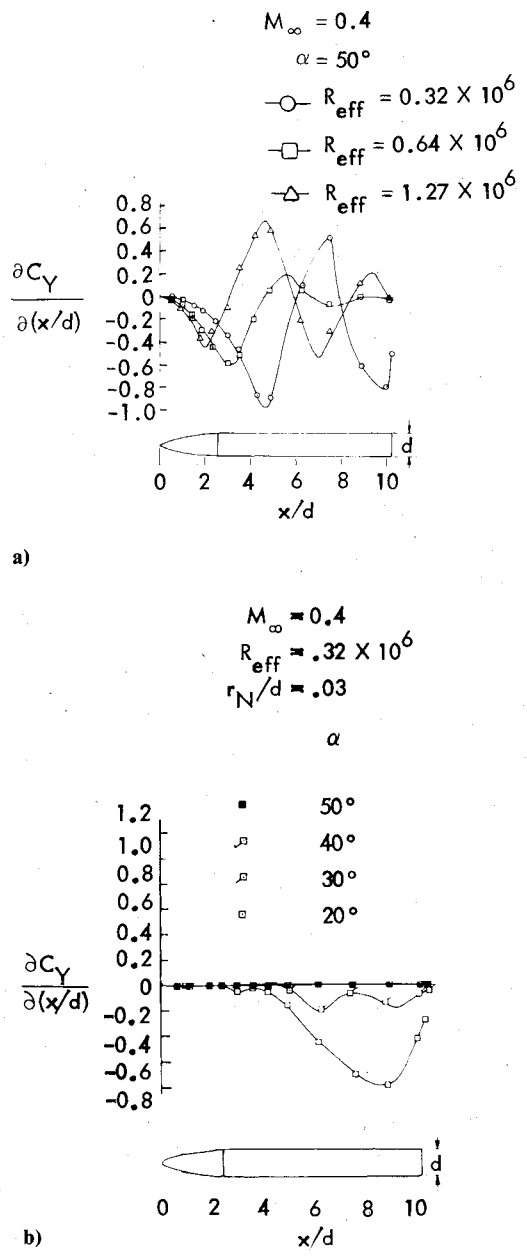

Fig. 10 Effect of angle of attack on side force distribution on a) pointed ogive-cylinder and b) blunted ogive-cylinder.[24]

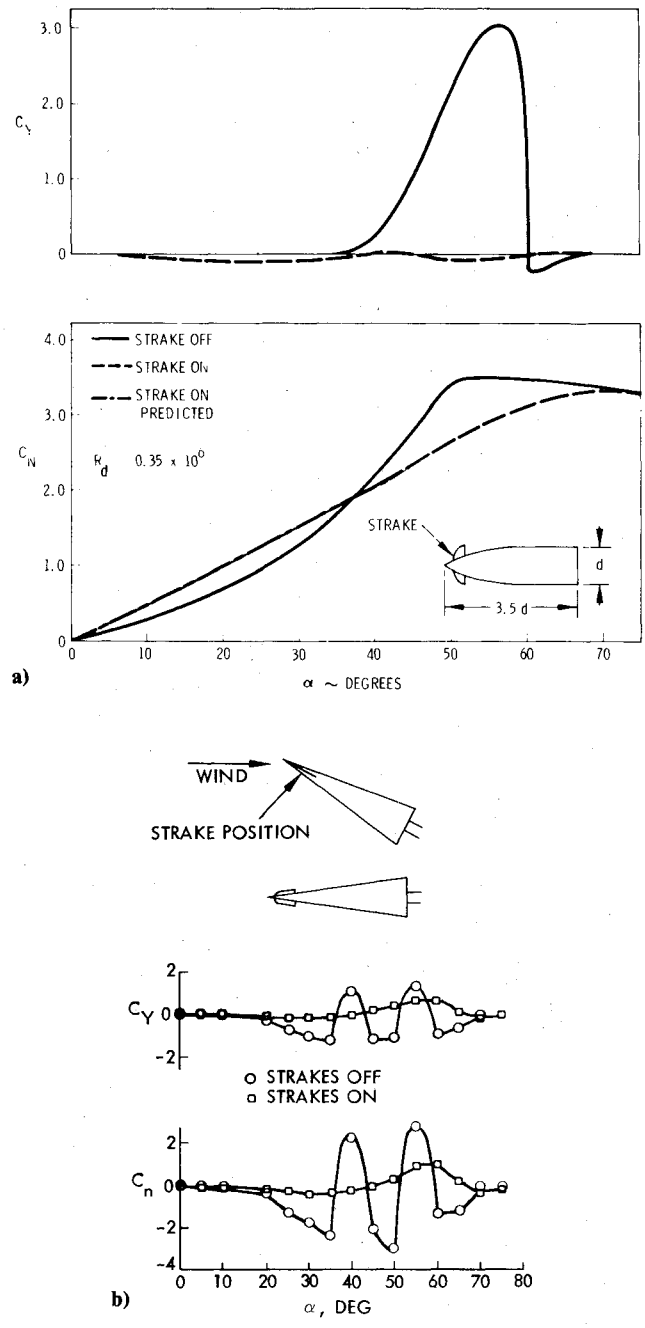

Fig. 11 Effect of nose strake on vortex-induced loads on a) pointed ogive-cylinder and b) sharp cone.[20]

angle of attack with attendant large $|C_Y|_{max}$. This is demonstrated by the results[24] in Fig. 10 and is also indicated by the data in Ref. 20. Thus, it would appear that for very long vehicles, such as sounding rockets, a very slender, pointed nose will give the smallest $|C_Y|_{max}$, whereas on an aircraft or shorter missile body a rounded nosetip will give the minimum $|C_Y|_{max}$.

While the use of such alleviation devices as the nose boom and nose bluntness may have been prompted by other considerations than concern for vortex-induced side loads, strakes have always been used for the expressed purpose of side load alleviation.[2,3,12,15,20,25] The design used by Coe et al.[20] seems to work well for the $l/d=3.5$ tangent ogive (Fig. 11a) but to be somewhat less effective on a cone with its smaller apex angle (Fig. 11b). The strake does not extend all the way to the tip, thus leaving room for the birth of asymmetric vortices. The action of the strake may then be somewhat similar to that of too short a splitter plate in the two-dimensional case.[26] The splitter plate only extends the wake formation region and delays the start of the von Kármán vortex street, in this manner decreasing its frequency but not preventing the vortex street from being generated. Similarly, the results in Fig. 11b show that the strakes impede the formation of asymmetric vortices but do not prevent them from being formed. The results for the X-15 airplane[3] (Fig. 12) show something similar. The strakes do not go all the way to the nosetip, and, consequently, the left strake (Δ) does not have any larger effect than an undefined microscopic body asymmetry in the apex region (o). The strakes or body trips used by Brown[27] (Fig. 13) show the same trend, i.e., only the forward portion of the trip is effective in alleviating vortex-induced side loads, and the aft portion may actually increase the loads. The relative failure of the nose ring as a load alleviator is probably again due to the fact that vortices are allowed to be started at apex. All that the nose ring then can do is to interfere with the downstream formation, similarly to what the "set-back" strake did[20] (Fig. 11b).

An interesting variation of the conventional straight body trips are the helical trips developed by Rau[28] (Fig. 14). They

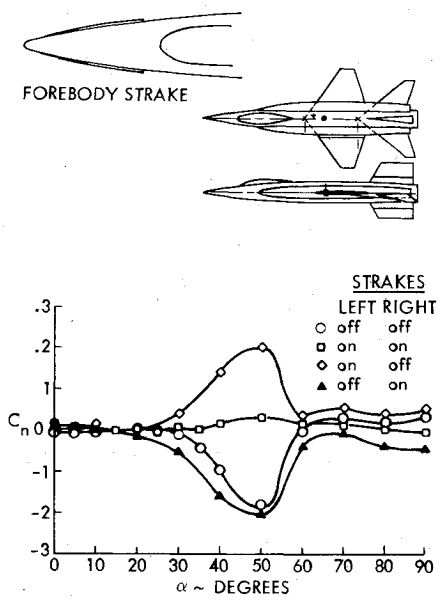

Fig. 12 Effect of nose strake on the vortex-induced yawing moment of the X-15 airplane.[3]

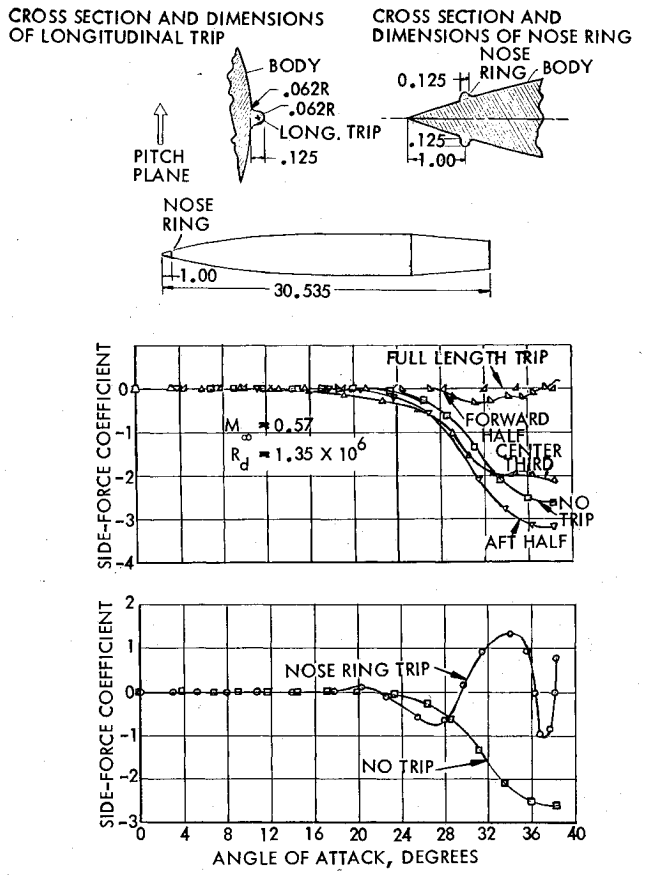

Fig. 13 Effects of body trips and nose ring trip on the vortex-induced side force.[27]

effectively eliminate the side force where the conventional trips fail. However, the helical trips do not "so disrupt the vorticity feeding mechanism at high angles of attack that the primary vortex pair could not be sustained." The flow pictures show that the vortices are sustained, and the normal force and pitching moment data (Fig. 15) tell the same story, i.e., the vortex-induced loads increase rather than decrease.

It is true that Scruton's helicals[29] do disrupt the Kármán vortex shedding on circular cylinders in two dimensional flow.

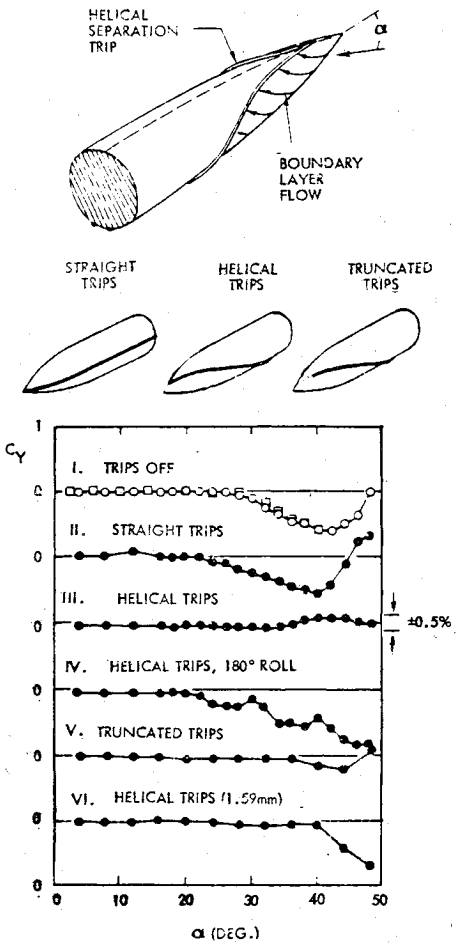

Fig. 14 Effect of helical and straight body trips.[28]

However, the concept cannot be carried over to three-dimensional flow in the manner suggested by Rau.[28] This is illustrated by the separated flow boundary measured on a pointed ogive-cylinder[30] (Fig. 16). A top view of the separation boundary is shown in Fig. 17.‡ It can be seen that the straight separation lines existing in the two-dimensional flow correspond to helical ones in the three-dimensional flow.

Comparing the separation geometry in Fig. 17 with the helical trip geometry in Fig. 14 one realizes that instead of disrupting the flow separation (with associated symmetric vortices) the helical trip reinforces the separation, moving it slightly upstream in the cross-flow plane, in this manner generating more vortex-induced lift in accordance with the experimental results in Fig. 15. In the nose region the distinction between a trip and a strake becomes diffuse, as any constant size body trip will act as a strake in some region near the apex. Reducing the trip wire diameter from 3.18 mm to 1.59 mm degraded greatly the trip or strake effectiveness (Fig. 14). The incipient asymmetric vortex-shedding was delayed from $\alpha = 25$ deg to $\alpha = 40$ deg, but the maximum side load finally reached at $\alpha = 50$ deg was of the same magnitude as for the basic (no-trip) body.

Whereas a body strake generates its own vortices, thereby being able to generate an asymmetric vortex pair regardless of the Reynolds number, the body trip acts only via its tripping action on the boundary layer. Its location relative to the natural separation line is, therefore, crucial. This is illustrated by the body trip data in Figs. 13 and 14, showing that the straight trip is efficient at supercritical conditions,[27] $R_d = 1.35 \times 10^6$ (Fig. 13) but not at critical flow conditions,[28] $R_d = 0.47 \times 10^6$ (Fig. 14). At the critical Reynolds number of

‡The lateral scale is expanded four times in relation to the axial scale to make the separation boundary better defined.

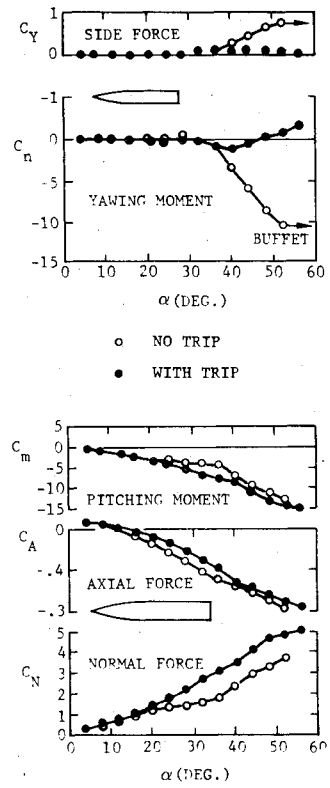

Fig. 15 Effect of helical trips on vortex-induced aerodynamic characteristics.[28]

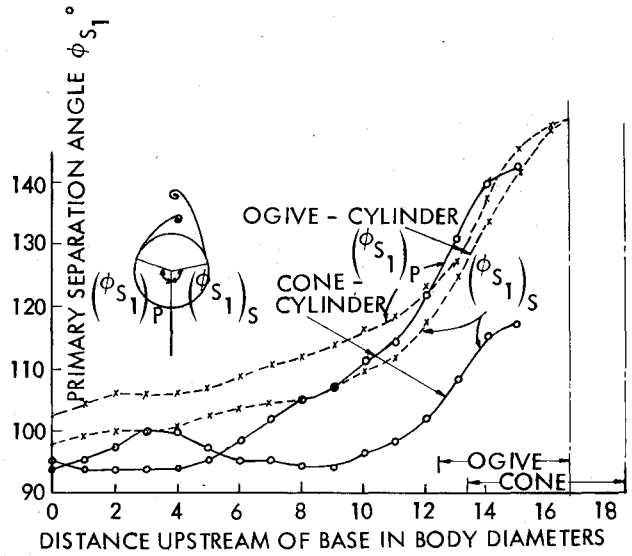

Fig. 16 Separation lines on cone-cylinder and ogive-cylinder at $M_\infty = 0.6$ and $R_d = 1.9 \times 10^6$ (Ref. 30).

Rau's test[28] subcritical separation can occur on one side and supercritical on the other, thereby generating the maximum vortex-induced side force.[8,9] Thus, a fix would be to force the supercritical separation towards the subcritical position, resulting in symmetric subcritical separation. The force data in Fig. 15 confirm that the helical trip indeed changes flow conditions towards the subcritical condition. Not only does the trip effectively eliminate the vortex-induced side force and side moment but it also increases normal and axial forces and generates a more stabilizing pitching moment. The increased normal force (with associated improvement of the static stability) is a result of the increased cross-flow drag for subcritical conditions, and the axial force increase is due to the associated loss of suction on the pointed forebody.

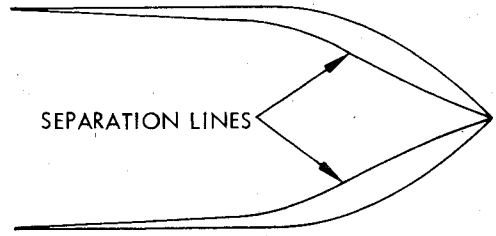

Fig. 17 Exploded view of flow separation geometry on ogive-cylinder.

The sketches in Fig. 18 illustrate why the helical trip might work at these test conditions, while the straight trip does not. Without a trip the critical conditions sketched in the left part of the figure are expected at this Reynolds number. In the middle is illustrated how the helical trip may work. Forward of section A-A it works as a regular separation device, forcing separation to take place at the trip. However, at and behind section A-A it acts as a preseparation device.[31] In this particular case it is not delaying separation but delaying boundary-layer transition. The effective Reynolds number of the reattaching flow is lessened because of the shortened approach length between reattachment and the lateral meridian, and subcritical separation takes place.

The straight, longitudinal trip, shown to the right in Fig. 18, was ineffective because of the near-critical Reynolds number. The trip will reinforce the subcritical separation already established through nose micro-asymmetries, but cannot move the supercritical separation on the opposite side to the subcritical position, as was the case for the helical trip. The reason is that the trip is not far enough upstream in the cross-flow plane to affect transition. Its preseparation effect will instead be to strengthen the turbulent boundary layer§ thereby reinforcing the supercritical flow separation on this side. Thus the straight trip will, if anything, aggravate the separation-asymmetry, as is also indicated by the measured side loads (see Fig. 14).

Thus, it appears that the conventional, lateral, straight body trip may work only outside the critical Reynolds number region. In contrast, it appears that it may be possible to position a helical body trip in such a manner that it would be effective at all Reynolds numbers.¶ The trip designed by Rau[28] may already have those characteristics. What is required is that it causes subcritical flow separation at subcritical and critical flow conditions, as just discussed, and through preseparation effects[31] strengthens the supercritical flow separation geometry at turbulent flow conditions, $R_d > 10^6$.

In regard to the relative merits of the various devices for side load alleviation one notices, of course, that nose bluntness is the simplest and works whether or not the vehicle flies coordinated maneuvers. Daniels[32] has shown that the effect of nose bluntness can be amplified by downstream diameter changes (backward facing steps and cylindrical cavities). Nose surface roughness is also likely to have a significant effect. For fixes such as strakes and body trips there may often be penalties to pay in regard to directional stability. Titiriga and Skow[22] show that although a regular nose strake can eliminate the vortex-induced side moment as well as their shark-nose design, the former will degrade directional stability while the latter actually enhances it.

The flow separation geometries on cone- and ogive-cylinders[30] (Fig. 16) point out a possible refinement in the use

§The low energy portion of the boundary layer is trapped in the local recirculation region of the separated flow, thereby strengthening the downstream boundary layer and delaying the flow separation and vortex formation.

¶But only in the correct azimuthal orientation. In the inverted position they have no effect, as they line up with the local streamlines (Fig. 14).

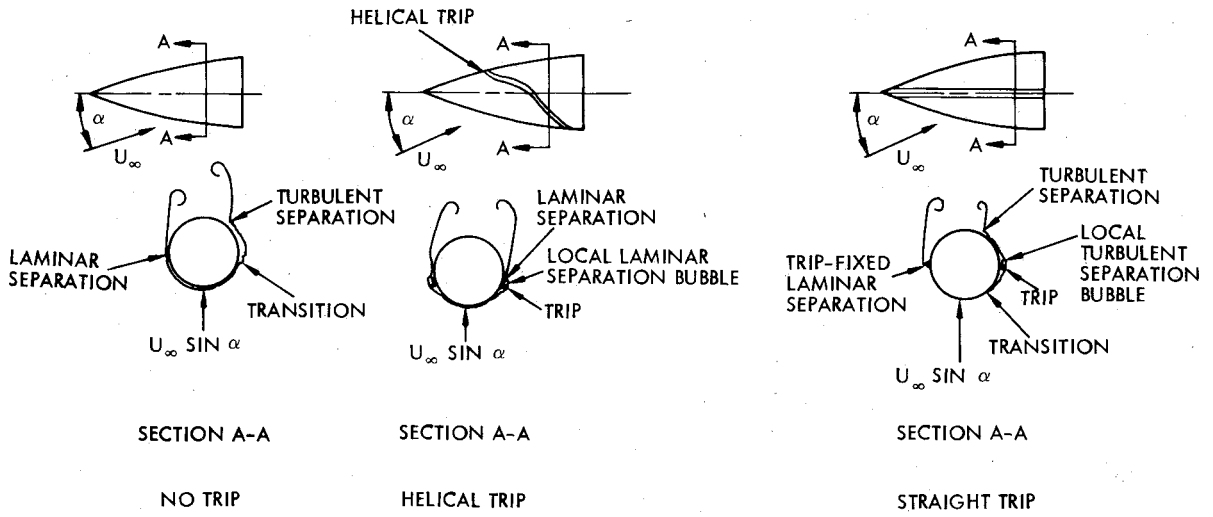

Fig. 18 Conceptual effect of body trips on flow separation.

of nose bluntness. If one substitutes the tip of the conic nose ($\theta_A = 5.8$ deg) by that of the ogival nose ($\theta_A = 13.8$ deg), one has reason to believe that this would cause the large nose-induced vortex-asymmetry to be reduced greatly or even disappear. Figure 6 and associated discussion showed that on a conic nose the maximum benefit is obtained with slightly less than 20% spherical nose bluntness. For an ogival nose the optimum nose bluntness would be somewhat higher. Thus, it may be advantageous to go to biconic and bi-ogival nose shapes to reduce the drag penalty associated with side load alleviation through nose bluntness.

Conclusions

A review of the existing data base in regard to alleviation of vortex-induced side loads has revealed the following:

1) Surface roughness has a large influence on the vortex-induced asymmetric loads. Invisible, microscopic irregularities in the nosetip region appear to control the asymmetric vortex shedding process, according to the observed effects of rolling the nosetip.

2) On a pointed slender body the vortex-induced asymmetric loads can be reduced greatly and sometimes eliminated completely by use of small nose bluntness, nose boom, nose strakes, or body trips. Whereas the two first devices have general applicability, the nose strakes and body trips are effective only for vehicles flying coordinated maneuvers.

More investigative efforts are needed to define in more detail the flow near apex. The cone data in Fig. 16 shows that tests on models that include only a portion of the cone or ogive body aft of the apex could reveal flow details otherwise not obtainable because of model size and Reynolds number limitations. The effect of roughness in the apex region would be of practical interest. Not only flight hardware type of roughness should be tested but also extreme roughness of the Jim-sphere type. If extreme roughness would bring the separation lines of the cone-cylinder in Fig. 16 toward those of the ogive-cylinder, extreme roughness would be a means of eliminating the large side loads. It is, of course, also possible that flight hardware type roughness may be extreme in relation to body and boundary layer dimensions near apex. In that case tests of subscale models with polished nosetips would be totally misrepresentative of full-scale flight conditions.

Finally, tests need to be performed to find out more about support interference and the possibility of minimizing if not eliminating it. The interference may come from bulky supports for wake probing instrumentation as well as from the model support itself. This problem can no longer be ignored as there is evidence indicating that much of the presently available experimental results for missiles and aircraft at high angles of attack is distorted by support interference.[11] Because of our complete dependence on experiments in this flight regime the problem of support interference must be solved before meaningful progress can be made.

Acknowledgments

The paper is based on results obtained in a study under Contract N60921-77C-0234 for the Naval Surface Weapons Center, Silver Spring, Md., under the direction of L. H. Schindel.

References

[1] Allen, H.J. and Perkins, E.W., "Characteristics of Flow Over Inclined Bodies of Revolution," NACA RM A50L07, 1951.

[2] Gowen, F.E. and Perkins, E.W., "A Study of the Effect of Body Shape on the Vortex Wakes of Inclined Bodies at a Mach Number of 2," NACA RM A53I17, Dec. 1958.

[3] Hassel, J.L., Jr. and Hewes, D.E., "Investigation of the Subsonic Stability and Control Characteristics of a 1/7 Scale Model of the North American X-15 Airplane With and Without Fuselage Forebody Strakes," NASA TM X-210, Feb. 1960.

[4] Thomson, K.D. and Morrison, D.F., "On the Asymmetric Vortex Shedding from Slender Cylindrical Bodies at Large Angles of Yaw," Weapon Research Establishment, Australia, Tech. Note HSA 106, May 1965.

[5] Fiechter, M., "Über Wirbelsysteme an schlanken Rotationskörpern und ihren Einfluss auf die aerodynamischen Beiwerte," Bericht 10/66, Dec. 1966, Deutsch-Französisches Forchungsinstitut, Saint Louis, France, Dec. 1966.

[6] Keener, E.R. and Taleghani, J., "Wind Tunnel Investigations of the Aerodynamic Characteristics of Five Forebody Models at High Angles of Attack at Mach Numbers from 0.25 to 2," NASA TM X-73, 076, Dec. 1975.

[7] McElroy, G.E. and Sharp, P.S., "An Approach to Stall/Spin Development and Test," AIAA Paper No. 71-772, July 1971.

[8] Reding, J.P. and Ericsson, L.E., "Maximum Vortex-Induced Side Force," *Journal of Spacecraft and Rockets,* Vol. 15, July-August 1978, pp. 201-207.

[9] Reding, J.P. and Ericsson, L.E., "Maximum Side Forces and Associated Yawing Moments on Slender Bodies," AIAA Paper 79-1647, AIAA Atmospheric Flight Mechanics Conference, Boulder, Colo., Aug. 6-8, 1979.

[10] AGARD FDP Meeting on Dynamic Stability Problems, AGARD CP-235, Athens, Greece, May 22-24, 1978.

[11] Ericsson, L.E., "A Summary of AGARD FDP Meeting on Dynamic Stability Parameters," Paper 2, AGARD Symposium on Stability and Control, AGARD CP-260, Ottawa, Canada, Sept. 25-28, 1978.

[12] Keener, E.R. and Chapman, G.T., "Onset of Aerodynamic Side Forces at Zero Sideslip on Symmetric Forebodies at High Angles of Attack," AIAA Paper 74-770, Aug. 1974.

[13] Nelson, R.C. and Fleeman, E.L., "High Angle of Attack Aerodynamics of a Slender Body with a Jet Plume," *Journal of Spacecraft and Rockets*, Vol. 12, Jan. 1975, pp. 12-16.

[14] Keener, E.R., Chapman, G.T., and Kruse, R.L., "Effects of Mach Number and Afterbody Length on Onset of Asymmetric Forces on Bodies at Zero Sideslip and High Angles of Attack," AIAA Paper 76-66, Jan. 1976.

[15] Keener, E.R., Chapman, G.T., Cohen, L., and Taleghani, J., "Side Forces on a Tangent-Ogive Forebody with a Fineness Ratio of 3.5 at High Angles of Attack and Mach Numbers from 0.1 to 0.7," NASA TM X-3437, Feb. 1977.

[16] Lamont, P.J. and Hunt, B.L., "Pressure and Force Distributions on a Sharp-Nosed Circular Cylinder at Large Angles of Inclination to a Uniform Subsonic Stream," *Journal of Fluid Mechanics*, Vol. 76, Part 3, Aug. 1976, pp. 519-559.

[17] Hunt, B.L. and Dexter, P.C., "Pressures on a Slender Body at High Angle of Attack in a Very Low Turbulence Level Airstream," Paper 17, AGARD CP-247, Jan. 1979.

[18] Skow, A.M., Titiriga, A., Jr., and Moore, W.A., "Forebody-Wing Vortex Interactions and Their Influence on Departure and Spin Resistance," Paper No. 6, AGARD CP-247, Jan. 1979.

[19] Pick, G.S., "Investigation of Side Forces on Ogive-Cylinder Bodies at High Angles of Attack in the M = 0.5 to 1.1 Range," AIAA Paper 71-570, June 1971.

[20] Coe, P.L., Jr., Chambers, J.R., and Letko, W., "Asymmetric Lateral-Directional Characteristics of Pointed Bodies of Revolution at High Angles of Attack," NASA TN D-7095, Nov. 1972.

[21] Whitehead, A.H., Jr. and Bertram, M.H., "Alleviation of Vortex-Induced Heating on the Lee Side of Slender Wings in Hypersonic Flow," *AIAA Journal*, Vol. 9, Sept. 1971, pp. 1870-1872.

[22] Titiriga, A. and Skow, A.M., "Analytical and Experimental Techniques to Predict Aircraft Dynamic Characteristics at High Angles of Attack," Paper No. 19, AGARD Meeting on Dynamic Stability Parameters, AGARD CP-235, Athens, Greece, May 22-24, 1978.

[23] Atraghji, E.G., "The Influence of Mach Number, Semi-Nose Angle, and Roll Rate on the Development of the Forces and Moments Over a Series of Long Slender Bodies of Revolution at Incidence," National Research Council, Ottawa, Canada, NAE Data Report 5 × 5/0020,1967.

[24] Dahlem, V. and Shereden, D., private communication of unpublished wind tunnel data, Flight Dynamics Laboratory, Wright-Patterson Air Force Base, Ohio, May 2, 1978 and Aug. 20, 1978.

[25] Chapman, G.T., Keener, E.R., and Malcolm, G., "Asymmetric Aerodynamic Forces on Aircraft Forebodies at High Angles of Attack—Some Design Guides," Paper No. 16, AGARD Meeting on Stall/Spin Problems of Military Aircraft, Ames Research Center, Moffett Field, Calif., Nov. 18-21, 1976.

[26] Apelt, C.J. and West, G.S., "The Effects of Wake Splitter Plates on Bluff-Body Flow in the Range $10^4 < R < 5 \times 10^4$, Part 2," *Journal of Mechanics*, Vol. 71, Part 1, 1975, pp. 145-160.

[27] Brown, R.C., "On the Asymmetrical Aerodynamic Forces of Slender Bodies of Revolution," Proceedings of BOWACA Meeting, McDonnell Aircraft Corp., St. Louis, Mo., 1965.

[28] Rau, D.M., "Side-Force Alleviation on Slender, Pointed Forebodies at High Angles of Attack," *Journal of Aircraft*, Vol. 16, Nov. 1979, pp. 763-768.

[29] Scruton, C. and Walshe, D.E., "A Means of Avoiding Wind-Exited Oscillations of Structures with Circular or Nearly-Circular Cross-Sections," Aeronautical Research Council, Great Britain, NPL-AERO-335, Oct. 1957.

[30] Rainbird, W.J., Crabbe, R.S., Peake, D.J., and Meyer, R.F., "Some Examples of Separation in Three-Dimensional Flows," *Canadian Aeronautics and Space Journal*, Vol. 12, Dec. 1966, pp. 409-423.

[31] Ericsson, L.E., "Aeroelastic Instability Caused by Slender Payloads," *Journal of Spacecraft and Rockets*, Vol. 4, Jan. 1967, pp. 65-73.

[32] Daniels, P., "Ogive Cylinder Modified for Near Minimum Side Moment," Paper 37, 11th Navy Symposium on Aeroballistics, NADC, Warminster, Pa., Aug. 1978.